Electronic Structure

PAPER

Structure and photophysics of rubrene–tetracene blends

To cite this article: Clemens Zeiser *et al* 2022 *Electron. Struct.* **4** 014002

IOP Publishing Electron. Struct. **4** (2022) 014002 https://doi.org/10.1088/2516-1075/ac47f2

Electronic Structure

RECEIVED
24 September 2021

REVISED
16 November 2021

ACCEPTED FOR PUBLICATION
4 January 2022

PUBLISHED
20 January 2022

PAPER

Structure and photophysics of rubrene–tetracene blends

Clemens Zeiser[1], **Adam J Berges**[2], **Tim Rammler**[3], **Frederik Munko**[1],
Alfred J Meixner[3], **Christopher J Bardeen**[2,*] **and Katharina Broch**[1,*]

[1] Institute of Applied Physics, University of Tübingen, Auf der Morgenstelle 10, 72076 Tübingen, Germany
[2] Department of Chemistry, University of California at Riverside, 501 Big Springs Road, Riverside, CA 92521, United States of America
[3] Institute of Physical and Theoretical Chemistry, University of Tübingen, Auf der Morgenstelle 18, 72076 Tübingen, Germany
[*] Authors to whom any correspondence should be addressed.

E-mail: christob@ucr.edu and brochkatharina@gmail.com

Keywords: singlet fission, time-resolved photoluminescence spectroscopy, organic semiconductors

Supplementary material for this article is available online

Abstract

The application potential of singlet fission (SF), describing the spontaneous conversion of an excited singlet into two triplets, underlines the necessity to independently control SF rates, energetics and the optical band gap. Heterofission, whereby the singlet splits into triplets on chemically distinct chromophores, is a promising approach to control the above-mentioned parameters, but its details are not yet fully understood. Here, we investigate the photophysics of blends of two prototypical SF chromophores, tetracene (TET) and rubrene (RUB) using time-resolved photoluminescence spectroscopy and time-correlated single photon counting to explore the potential for heterofission in combinations of endothermic SF chromophores.

1. Introduction

Singlet fission (SF) is the spontaneous conversion of a singlet exciton into two triplet excitons [1, 2]. Since it is a multi-exciton generation process, it has gained attention due to its potential for application in solar cells [3, 4]. Although SF has by now been observed in many different material classes [1] and significant progress has been made in the understanding of the process [2, 5–8], the development of new SF materials is complicated by the necessity to concurrently optimize the optical bandgap for efficient harvesting of solar photons, SF energetics for a reduction of energy losses during the conversion process, and the SF rate to avoid extensive losses by singlet energy transfer [9]. The ideal optical bandgap is given by the solar spectrum [10] and the SF rate is not only influenced by the SF energetics, but by several other key parameters that have been identified in the literature [2, 5, 6]. A challenge for application of SF is therefore an independent tuning of these parameters.

One way to achieve such a tuning is to combine two SF chromophores and enable heterofission, i.e., the conversion of a singlet into two triplets that are located at different types of chromophores [11]. Since the energy balance of heterofission is determined by the difference between the singlet energy ($E(S_1)$) and the sum of the triplet energies ($E(T_1)$) of the two molecules involved, it can be easily tuned by compound choice. Vice versa, for an active layer exploiting heterofission, the onset of absorption is determined by the compound with the lower optical band gap [12], independent of the choice of the second chromophore.

Heterofission has been observed in doped single crystals [11, 13], thin film blends [12] and heterodimers [14, 15] of pentacene (PEN) and tetracene (TET, figure 1(a)). In single- or polycrystalline blends involving an exothermic SF material such as PEN, heterofission can only be observed for low concentrations in the doping regime, since heterofission is otherwise either outcompeted by FRET or by the exothermic homofission [12]. This limits the applicability of the process in active layers of solar cells.

However, heterofission might become more efficient and, thus, observable even for mixing ratios closer to the equimolar ratio in blends of endothermic SF chromophores, in which the time scales of the homofission decay channels that compete with heterofission are slower. Prototypical candidates for such investigations are TET and rubrene (RUB, figure 1(b)). With the energy of S_1, $E(S_1) = 2.32$ eV, and the energy of T_1, $E(T_1)) = 1.25$ eV [16], SF in TET is endothermic by 180 meV. For RUB, the endothermicity of 30 meV

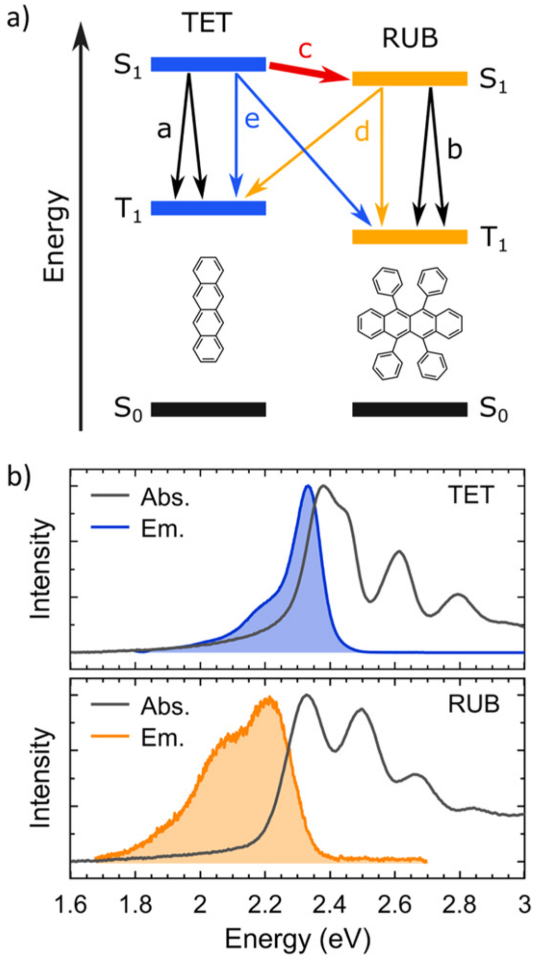

Figure 1. (a) Chemical structure of the molecules and schematic energy level diagram with possible bi-molecular relaxation pathways of the excited state: homofission of TET and RUB (a) and (b), energy transfer from TET to RUB (c) and heterofission (d) and (e). (b) Steady-state absorption and emission spectra of thin films of TET and RUB.

($E(S_1) = 2.27$ eV [17] and $E(T_1) = 1.15$ eV [17, 18]) is significantly smaller. SF in neat films and single crystals of both chromophores has been studied in detail [2, 6, 19–23] and direct emission from the triplet-pair state has been reported [6, 23]. The coupling between a Frenkel exciton and the triplet-pair state in RUB is strongly facilitated by symmetry-breaking vibrational modes [2, 6, 20]. This leads to the observation of emission from a triplet-pair state that is an intermediate state in the SF process in RUB [2, 6, 20].

Mixed with weakly interacting spacer molecules, TET [24] and RUB [25] exhibit a concentration dependent SF rate indicating the existence of incoherent population transfer from S_1 to the triplet-pair state. This observation is contrasted by reports of coherent SF in both materials [2, 20] and has be discussed to result from a high sensitivity of the excited state dynamics on sample preparation or by differences in time-resolution and sensitivity of the used experimental techniques [23]. While for TET there is a consensus that SF occurs in the order of 100 ps [6, 19, 23, 24], the details of the SF process are less clear for RUB [2, 6, 20, 27, 28]. In the following we adopt the assignment of reference [6] with the formation of ^{1}(TT) on the order of 30 ps and the triplet separation on the order of nanoseconds.

The aim of our study is to investigate if heterofission can be observed in mixed films of TET and RUB. For TET singlets, heterofission might be favoured against homofission by a reduced endothermicity (80 meV) of the SF process due to the addition of RUB with an energy of T_1 that is 100 meV below $E(T_1)$ of TET and heterofission of an excited RUB singlet has with 130 meV an only slightly more unfavourable energy balance. Heterofission should be observable by an enhanced TET singlet decay rate and a quenching of RUB emission. For this study, we co-deposit both materials and probe the resulting excited state dynamics using time-resolved photoluminescence spectroscopy (TRPL) and time-correlated single photon counting (TCSPC). Due to the differences in molecular geometry and molecular arrangement in thin films [29], a phase separation into domains of neat TET and neat RUB is likely to occur upon co-deposition. However, the large exciton diffusion lengths reported for both materials [30, 31] will enable singlet excitons formed within the domains of either compound to reach the interfaces between those domains and to undergo additional bi-molecular relaxation processes such as energy transfer and heterofission, see figure 1(a) for a schematic summary of bimolecular relaxation processes. Thus, we expect a complex excited state dynamics of the heterostructures after photoexcitation.

2. Methods

Mixed films of TET (Sigma Aldrich, 98%) and RUB (Sigma Aldrich, 98%) were grown by organic molecular beam deposition on silicon with a native oxide layer (Microchemicals) and on borofloat glass substrates (JGS1, Microchemicals) at a base pressure of 1×10^{-8} mbar. The total growth rate was 0.6 nm min^{-1}, with the rates of the two materials monitored separately by two quartz crystal microbalances, calibrated using x-ray reflectivity. The final film thickness was 80 nm. UV–vis transmission spectra were measured using a Perkin Elmer Lambda 950 spectrophotometer. X-ray reflectivity was measured on a diffractometer (3303TT, GE) using Cu K_α-radiation ($\lambda = 1.5406$ Å) and a 1D detector (Meteor 1D, XRD Eigenmann). GIWAXS measurements were performed using an in-house wide-angle x-ray scattering setup (Xeuss 2.0, Xenocs) with $\lambda = 1.5406$ Å and a Pilatus 300k detector.

TRPL measurements were taken with a Hamamatsu C4334 streakscope having a time resolution of 20 ps and a spectral resolution of 2.5 nm. The 800 nm output of an 80 MHz coherent Vitesse Ti:Sapphire oscillator was frequency doubled to generate the 400 nm excitation pulse. A Pockels cell controlled by a ConOptics pulse-picking system was used to adjust the repetition rate of the oscillator to 100 kHz. A 450 nm long wavepass filter was placed before the streak camera to minimise the contribution of laser scatter to the signal. All measurements were performed in a vacuum cryostat (10^{-5} torr) fitted with optical windows, and pulse fluences remained below 1.2 μJ cm^{-2}.

The TCSPC and steady-state PL measurements were conducted with a pulsed laser diode LDH-P-C-470 (Pico-Quant, Germany) of 470 nm wavelength, a time-averaged power of 0.05 μW and a repetition rate of 40 MHz. Using a Plan-NEOFLUAR 65x/NA 0.75 air-objective (Carl Zeiss AG, Germany), the laser pulses were focused on a spot with 30 μm diameter on the sample, yielding a fluence of 1.77×10^{-4} μJ cm^{-1} [2]. For TCSPC, emitted photons were detected with an electron multiplying iXon Ultra 888 EMCCD camera (Andor Technology, UK). The Andor Solis software was used for controlling the camera and further data analysis including fits with a convolved IRF. For steady-state PL spectroscopy, an Acton SP300 spectrometer with a PIXIS 100 camera (both Princeton Instruments, USA) was used.

3. Results

Comparing the steady-state optical properties of the two compounds in neat films (see figure 1(b)), a clear impact of the difference in molecular arrangement can be seen. TET forms a herringbone arrangement in thin films [29] with two molecules per unit cell. The coupling of translationally inequivalent transition dipole moments leads to a Davydov-splitting of the energetically lowest transition around 2.4 eV. In contrast, thin films of RUB are amorphous without pronounced long range order [17] and the absorption spectrum resembles the solution spectrum [17].

For our study, we prepared a series of RUB:TET blends with different mixing ratios between 5% and 90% RUB concentration. The steady-state absorption spectra of the blends [see supporting information (https://stacks.iop.org/EST/4/014002/mmedia), SI] can be described as a superposition of the absorption spectra of the neat compounds, in agreement with the expected phase separation. This is further confirmed by grazing incidence wide-angle x-ray diffraction (GIWAXS), see figure 2. For the blends with 10% and 20% RUB concentration, diffraction rings with radii of $q = 0.51$ Å^{-1}, $q = 0.87$ Å^{-1}, $q = 1.26$ Å^{-1} and $q = 1.36$ Å^{-1} are observed, which can be assigned to diffractions from the (001), (011), (111) and (110) lattice planes of the TET bulk polymorph [29], respectively. Notably, the (001) reflection (observed for neat TET around $q_z = 0.55$ Å^{-1} and close to $q_{xy} = 0$ Å^{-1}) is observed in these blends with an additional maximum rotated by about 20° towards q_{xy}, which denotes a slight rotation of the TET crystallites relative to the substrate plane compared to the crystallites in neat TET films. For the 50% RUB blend, all reflections become weaker, and those corresponding to the (011) and the (111) lattice planes disappear. Finally, for the blends with 80% and 90% RUB concentration, a complex pattern is observed. Some of the maxima are located on rings ($q = 0.54$ Å^{-1}, $q = 0.89$ Å^{-1}, $q = 1.25$ Å^{-1}) that can again be assigned to reflections from the (001), (011) and (111) lattice planes of TET, yet with a markedly different orientation compared to those in the blends with 10% and 20% RUB concentration as indicated by the differences in position of the Bragg-reflexes along those rings. In addition, a diffraction ring with a radius of $q = 0.96$ Å^{-1} is observed. This value matches reflections at the (011) lattice planes of the RUB single crystal structure [32] and indicates the existence of phase separated RUB domains. We note that also reflections at the (002) lattice planes of the TET thin film polymorph [29] are

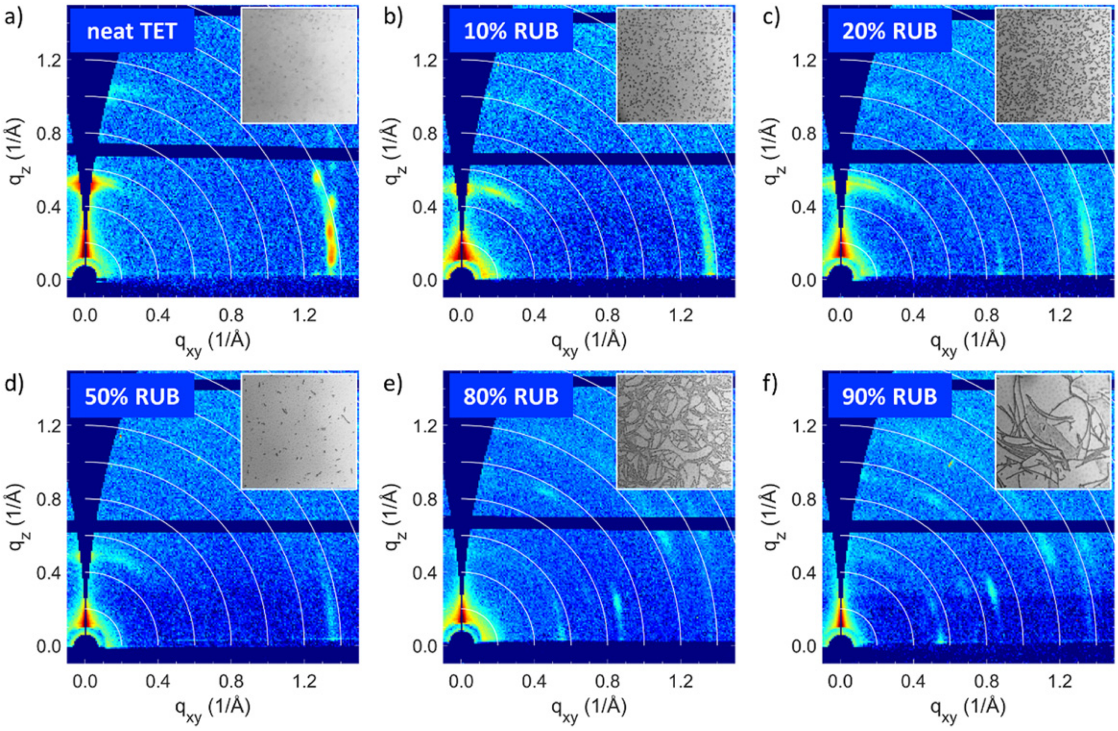

Figure 2. Reciprocal space maps measured by GIWAXS and optical microscopy images (insets) of RUB:TET blends. The white circles with a spacing of 0.2 Å^{-1} are guides to the eye.

expected at this position, but since the corresponding reflection at the (001) lattice planes cannot be observed, we exclude this possibility here.

Optical microscopy images of the blends are shown as insets in figure 2. For low RUB concentrations, we observe small, dark spots which increase in number with increasing RUB concentration. In the equimolar blend, the number of dark spots suddenly drops which we interpret either as the onset of dendrite formation, with the coalescence of RUB domains into large and tall features or as being caused by the sudden decrease in the long-range order as indicated by the reduced Bragg-peak intensity in the GIWAXS data. The latter might result from increased strain due to the coexistence of a similar number of TET and RUB domains. Images for higher RUB concentrations are dominated by large dendrites as observed before in neat RUB films [33]. In summary, the GIWAXS and microscopy data corroborate the formation of pure domains of the two compounds in RUB:TET blends. We will refer to these phase separated domains as RUB and TET domains in the following discussion, although the incorporation of a few guest molecules of RUB (TET) in TET (RUB) domains cannot be excluded.

To probe the excited state dynamics, we performed TRPL and TCSPC experiments using an excitation energy of 3.1 eV (TRPL) and 2.64 eV (steady state PL and TCSPC), respectively, which are both above the band gap of both compounds. The TCSPC data are shown along with steady-state PL spectra in figures 3(a) and (b). Before discussing the time-resolved decay of the PL intensity, we focus on the time-integrated PL spectra of the blends in ascending order of RUB concentration. While the PL spectra of blends with RUB concentrations of 20% and below are clearly dominated by TET emission, the spectrum of the equimolar blend can be described as a superposition of the contributions of TET and RUB (see SI). Further increasing the RUB concentration to 80% and 90% leads to the observation of an additional spectral feature at 1.95 eV. This new feature could arise due to emission from the ^{1}(TT) state in crystalline RUB domains [6]. If this is the case, it is surprising that a similar spectral feature cannot be observed for the neat RUB sample. But neat RUB is amorphous, while the presence of TET clearly facilitates the formation of crystallites in the blends as indicated by the Bragg-peaks observed in the GIWAXS-data (figure 2), which may allow the observation of ^{1}(TT) emission of RUB. Alternatively, the 1.95 eV feature could reflect a RUB-TET pair state, for example an exciplex. In either case, this emission shows that there exist new excited state relaxation pathways in the blends.

For the analysis of the excited state dynamics, we fitted the temporal evolution of the intensity decay by a convolution of a biexponential function and the instrument response function (IRF, see figure 3(c)). For both neat compounds, the multiexponential decay agrees with literature [6, 19, 23, 24, 27, 28]. In TET, the initial fast decay with a rate of 8.0 ns^{-1} can be assigned to SF [19, 23, 24], while neat RUB exhibits a much slower, biexponential PL decay with rates of 0.91 ns^{-1} and 3.6 ns^{-1} and a 53% relative amplitude of the faster decay

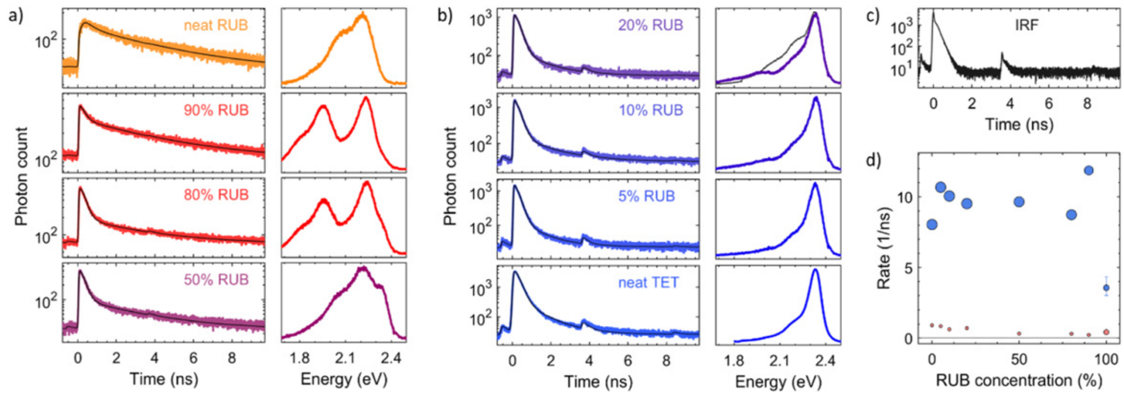

Figure 3. (a) and (b) TCSPC data, biexponential fits (black lines) and steady-state PL spectra of RUB:TET blends. (c) Instrument response function (IRF) of the TCSPC measurements. (d) Decay rates obtained by biexponential fits to the TCSPC data shown in (a) and (b). The marker size represents the amplitude of the decay rate. For the calculation of the model spectrum in the 20% RUB panel in (b) (thin black line), see SI.

Table 1. Decay rate associated with the SF process (short singlet decay time) for different RUB concentrations.

RUB (%)	0	5	10	20	50	80	90	100
r (ns^{-1})	8.03	10.68	10.05	9.52	9.65	8.73	11.87	3.56

[28], see figure 3(a). We assign the biexponential PL decay in RUB to a decay in S_1 population caused by the conversion of S_1 to ^{1}(TT), and subsequent separation of ^{1}(TT) [6, 27].

Comparing the temporal evolution of the PL intensity of the blends with those of the neat compounds, we can assign the initial short decay in the blends with TET excess to the relaxation of TET singlets. Even for the blends with RUB excess the fast dynamics is likely to result from TET singlets, as RUB exhibits in our data a much slower dynamics, dominating the spectrum at late times (see SI). We find that the larger decay rate of the excited state, which can be assigned to SF, is consistently increased (compare figure 3(d)). This contrasts with previous reports of the dynamics TET or RUB in blends with weakly interacting molecules [25, 26] for which a reduction of the rates was found and will be discussed in detail below. Between the blends, the results (figure 3(d) and table 1) show no clear trend with changing RUB concentration, which is consistent with the phase separation into neat domains indicated by our structural investigations.

4. Discussion

For the discussion of possible origins of the curious increase of the SF rate in the blends compared to the neat films, we first summarize the photophysical processes involved in the relaxation of excited states. Besides radiative relaxation and SF of singlets on TET and singlets on RUB, the presence of interfaces between TET and RUB domains opens new, diffusion-mediated, relaxation channels. The corresponding processes include energy transfer from TET to RUB, heterofission of TET singlets and heterofission of RUB singlets, leading to triplets on TET and RUB, respectively.

If the RUB and TET domains did not interact at all, then the PL lifetimes and spectra of all samples could be described by a simple weighted superposition of both pure compounds. This seems to be the case for the equimolar RUB:TET blend, which can be described by a superposition of contributions of both compounds, see SI. However, down-scaling this superposition spectrum to fit the intensity of the PL spectrum of the 20% blend and comparing it to the experimental PL spectrum (figure 3(b)), there is less emission in the low energy region than predicted. If the 1.95 eV feature is due to the RUB 1(TT) state, its absence may indicate the growth of diffusion-mediated additional relaxation channels as the interface area between RUB and TET domains is increased in blends with low RUB concentrations. Since RUB has the smaller band gap, energy transfer to TET is unlikely and the quenching could thus be caused either by trapping of RUB singlet states at grain boundaries and defects [23] or by heterofission at the interface to TET domains. The latter process could also explain the increased decay rate of TET singlets in the blends with RUB concentrations of 50% or less, although here energy transfer would be an alternative decay channel. This energy transfer from TET to RUB, however, should result in increased emission of RUB. As mentioned above, a decrease in RUB emission is actually observed for these concentrations instead. The slight increase in the TET PL decay rates at low RUB concentrations, along with the lack of a concomitant increase in RUB emission, are both consistent with heterofission playing a role in the photophysics. For the ultrathin samples used in these experiments, PL spectroscopy is especially well suited to probe such heterogeneous processes occurring at interfaces of SF chromophores, especially if triplet-pair state emission can be observed.

5. Conclusion

To summarize, we presented a TRPL study of phase separating blends of the two prototypical endothermic SF chromophores RUB and TET. While our data indicate that independent singlet decay channels exist in equimolar blends, the increased interface area in blends with reduced RUB concentration led to a quenching of RUB emission and a slightly increased decay rate of the TET singlet, which gives preliminary evidence for diffusion-mediated heterofission despite phase separation in these heterostructures. This is a first step towards the independent tuning of SF energetics and optical band gap of active layers in solar cells based on heterostructures of endothermic SF chromophores.

Acknowledgments

CZ and KB thank Professor Schreiber (University of Tübingen) for access to equipment. Financial support by the German Research Foundation (BR4869/4-1) is gratefully acknowledged. CJB acknowledges support by the US National Science Foundation, Grant CHE-1800187.

Data availability statement

All data that support the findings of this study are included within the article (and any supplementary files).

ORCID iDs

Alfred J Meixner https://orcid.org/0000-0002-0187-2906
Katharina Broch https://orcid.org/0000-0002-9354-292X

References

[1] Smith M B and Michl J 2010 *Chem. Rev.* **110** 6891
[2] Miyata K, Conrad-Burton F S, Geyer F L and Zhu X-Y 2019 *Chem. Rev.* **119** 4261
[3] Congreve D N *et al* 2013 *Science* **340** 334
[4] Jadhav P J *et al* 2012 *Adv. Mater.* **24** 6169
[5] Bakulin A A, Morgan S E, Kehoe T B, Wilson M W B, Chin A W, Zigmantas D, Egorova D and Rao A 2016 *Nat. Chem.* **8** 16
[6] Yong C K *et al* 2017 *Nat. Commun.* **8** 15953
[7] Dover C B, Gallaher J K, Frazer L, Tapping P C, Petty A J, Crossley M J, Anthony J E, Kee T W and Schmidt T W 2018 *Nat. Chem.* **10** 305
[8] Bossanyi D G *et al* 2021 *Nat. Chem.* **13** 163
[9] Einzinger M *et al* 2019 *Nature* **571** 90
[10] Hanna M C and Nozik A J 2006 *J. Appl. Phys.* **100** 074510
[11] Geacintov N E, Burgos J, Pope M and Strom C 1971 *Chem. Phys. Lett.* **11** 80395
[12] Zeiser C, Moretti L, Lepple D, Cerullo G, Maiuri M and Broch K 2020 *Angew. Chem., Int. Ed.* **59** 19966
[13] Burgos J, Pope M, Swenberg C E and Alfano R R 1977 *Phys. Status Solidi* B 83
[14] Sanders S N, Kumarasamy E, Pun A B, Steigerwald M L, Sfeir M Y and Campos L M 2016 *Angew. Chem., Int. Ed.* **55** 3373
[15] Pun A B, Asadpoordarvish A, Kumarasamy E, Tayebjee M J Y, Niesner D, McCamey D R, Sanders S N, Campos L M and Sfeir M Y 2019 *Nat. Chem.* **11** 821
[16] Tomkiewicz Y, Groff R P and Avakian P 1971 *J. Chem. Phys.* **54** 4504
[17] Irkhin P, Ryasnyanskiy A, Koehler M and Biaggio I 2012 *Phys. Rev.* B **86** 085143
[18] Ryasnyanskiy A and Biaggio I 2011 *Phys. Rev.* B **84** 193203
[19] Burdett J J, Gosztola D and Bardeen C J 2011 *J. Chem. Phys.* **135** 214508
[20] Breen I, Tempelaar R, Bizimana L A, Kloss B, Reichman D R and Turner D B 2017 *J. Am. Chem. Soc.* **139** 11745
[21] Chan W-L, Ligges M and Zhu X-Y 2012 *Nat. Chem.* **4** 840
[22] Cruz C D, Chronister E L and Bardeen C J 2020 *J. Chem. Phys.* **153** 234504
[23] Tayebjee M J Y, Clady R G C R and Schmidt T W 2013 *Phys. Chem. Chem. Phys.* **15** 14797
[24] Zeiser C, Cruz C, Reichman D R, Seitz M, Hagenlocher J, Chronister E L, Bardeen C J, Tempelaar R and Broch K 2021 *Nat. Commun.* **12** 5149
[25] Tian X, Zhou L, Chen X, Meng Y, Xiong Z, Zhou X and Zhang Y 2017 *Org. Electron.* **50** 429
[26] Sher P-H, Chen C-H, Chiu T-L, Lin C-F, Wang J-K and Lee J-H 2019 *J. Phys. Chem.* C **123** 3279

[27] Piland G B, Burdett J J, Kurunthu D and Bardeen C J 2013 *J. Phys. Chem.* C **117** 1224

[28] Nahm R K and Engstrom J R 2017 *J. Chem. Phys.* **146** 052815

[29] Irkhin P and Biaggio I 2011 *Phys. Rev. Lett.* **107** 017402

[30] Berghuis A M, Raziman T V, Halpin A, Wang S, Curto A G and Rivas J G 2021 *J. Phys. Chem. Lett.* **12** 1360

[31] Jurchescu O D, Meetsma A and Palstra T T M 2006 *Acta Crystallogr.* B **62** 330

[32] Wang L, Li Y, Zou F, Du H, Sun L, Zhang J, Song X and Song G 2016 *RSC Adv.* **6** 3532